Available online at www.sciencedirect.com
SCIENCE DIRECT®
Journal of Power Sources 115 (2003) 295–304
JOURNAL OF POWER SOURCES
www.elsevier.com/locate/jpowsour

# Effect of glass–ceramic filler on properties of polyethylene oxide–$LiCF_3SO_3$ complex

C.J. Leo[a], A.K. Thakur[b,1], G.V. Subba Rao[a], B.V.R. Chowdari[a,*]

[a]*Department of Physics, National University of Singapore, Singapore 119260, Singapore*
[b]*Department of Physics, North Eastern Regional Institute of Science and Technology, Itanagar (Nirjuli) 791109, India*

Received 3 October 2002; accepted 12 December 2002

**Abstract**

Lithium-ion conducting composite polymer electrolytes (CPE),$(PEO)_8$–$LiCF_3SO_3$ (PEO = polyethylene oxide) dispersed with a glass–ceramic, $Li_{1.4}[Al_{0.4}Ge_{1.6}(PO_4)_3]$ as a filler have been prepared as films and their thermal, mechanical, electrical and electrochemical properties have been studied. The glass transition temperature increases with filler addition reaches a maximum value of −39 °C for $x = 7.5$ wt.%, and then decreases. Enhancement in the electrochemical stability of the films is noted; a maximum working voltage of 3.75 V is found at $x = 10$ wt.%. Addition of filler decreases the ionic conductivity for $x = 7.5$ wt.%, $\sigma = 1.6 \times 10^{-7}$ S cm$^{-1}$ which is a factor three lower than that for the PS complex. The $E_a$ and $\log_{10}(\sigma_0)$ values of the composite polymer electrolytes consistently decrease with increasing $x$. The mechanical properties are enhanced with filler addition, a maximum tensile strength of 22.8 MPa, is obtained at $x = 7.5$–10 wt.%, a value which is three times higher than that for the PS complex.


*Keywords:* Composite polymer electrolytes; Ionic conductivity; Glass-transition temperature; Tensile strength; Breakdown voltage; Lithium-ion

## 1. Introduction

Solid polymer electrolytes, in thin film form, have attracted attention ever since their development [1] and subsequent recognition as materials of technological importance in solid-state electrochemical devices [2–6]. But solid polymeric electrolytes, such as complexes of polyethylene oxide (PEO) with metal salts, attain useful ionic conductivity only at temperatures ($T$) above 60–70 °C, i.e. at their transition temperature from the crystalline to amorphous phase. Polymer–salt (PS) complexes, above this $T$-range, behave as viscous liquids with poor mechanical properties. As a result, the use of conventional polymeric electrolytes in devices poses problems such as leakage and loss of electrode–electrolyte contact, as encountered in devices based on liquid electrolytes. Hence, to improve the physical, mechanical and ion-conducting properties of the polymeric electrolytes, several techniques have been adopted, e.g. formation of block copolymers [7,8], use of grafting [9,10] and dispersion of micro/nano-sized ceramic particles into the PS complex matrix as the third component. The last mentioned approach, first suggested by Steele and Weston [11], is simple and the solid complexes so obtained are known as the composite polymer electrolytes (CPEs). Since then, there have been reports of the addition of a number of inorganic ceramic fillers such as $Al_2O_3$, $TiO_2$, $SiO_2$, $Li_3N$, $LiAlO_2$, and fast ionic conductors (FIC) based on the Nasicon structure to the PS complex, $(PEO)_n$–Li-salt [12–19]. The effect of these additives in CPEs has two antagonistic effects: (i) Enhancement of the volume fraction of the amorphous phase in the polymer complex that supporting the ion transport process; (ii) increase in the glass transition temperature ($T_g$) that suppresses the polymer chain motion responsible for ion transport. The ceramic additives cause however, other desirable changes in the CPEs such as improvement in mechanical and thermal stability [19–22] and enhancement in the electrochemical and interfacial properties [19,23–25]. These features render CPEs suitable for practical application in devices.

The present study examines the effect of addition of the ionically conducting glass–ceramic, $Li_{1.4}[Al_{0.4}Ge_{1.6}(PO_4)_3]$, as a filler in the PEO–$LiCF_3SO_3$ complex. Being a FIC with an ionic conductivity of $\sim 10^{-4}$ S cm$^{-1}$ at room temperature [26–28], this filler is expected to act as an active component of the CPE and also provide other desirable physical, thermal, mechanical and electrochemical properties.

* Corresponding author. Fax: +65-777-6126.
*E-mail address:* phychowd@nus.edu.sg (B.V.R. Chowdari).
[1] The work was done when the author was at N.U.S., Singapore.

0378-7753/03/$ – see front matter © 2003 Elsevier Science B.V. All rights reserved.
doi:10.1016/S0378-7753(03)00007-7

## 2. Experimental

### 2.1. Synthesis

The standard 'solution-cast' technique was used to prepare CPE films of thickness 150–250 μm. Commercial PEO (Aldrich; molecular weight: $\sim 6 \times 10^5$) was used as the polymer host matrix. Lithium triflate, ($LiCF_3SO_3$ (Fluka)), was vacuum dried at 10 °C prior to use. The glass–ceramic filler, $Li_{1.4}[Al_{0.4}Ge_{1.6}(PO_4)_3]$, was synthesized by first melting the precursors ($Li_2CO_3$, $Al_2O_3$, $GeO_2$ and $(NH_4)H_2PO_4$) at 1400 °C and then quenching on to a stainless-steel plate with a steel hammer. The resulting glass flakes were then given two stages of heat treatment, namely, 625 °C for 2 days followed by 625 °C for 4 days. The resulting glass–ceramic pieces were ground to fine powder (size 2–5 μm) and characterized by X-ray diffraction. The appropriate ratios of PEO and $LiCF_3SO_3$ were dissolved in dehydrated acetonitrile separately and the solutions were mixed and stirred thoroughly for 12 h. Different weight percentages of the glass–ceramic filler were then added to the solution which was stirred for a further 12 h. The resulting dispersed solutions were then cast in glass petri dishes and allowed to evaporate slowly at room temperature (25 °C). The CPE films so prepared were then dried under vacuum at 40 °C for 3–4 days to remove any residual solvent (acetonitrile).

The PEO:$LiCF_3SO_3$ molar ratio was maintained at 8:1 and the amount of filler, $Li_{1.4}[Al_{0.4}Ge_{1.6}(PO_4)_3]$, dispersed is expressed as a weight percent (wt.%) with respect to the host polymer (PEO): $x\% = (\text{wt. of filler}/\text{wt. of PEO}) \times 100$. Thus, the compositions of the CPE films are represented as: $(PEO)_8$–$LiCF_3SO_3 + x$ wt.% $Li_{1.4}[Al_{0.4}Ge_{1.6}(PO_4)_3]$, where $x = 0$, 1, 2, 5,7.5, 10, 15, 20 and 25.

### 2.2. Characterization

The optical microscopy of the CPE films was examined using a computer-controlled image analysis system (Olympus optical microscope, Model: BX 60). The X-ray diffraction (XRD) studies of the ceramic filler and the CPEs were performed using Philips X'PRT–MPD system (Cu $K_\alpha$ radiation; $2\theta$: 10–50°). Differential scanning calorimetry (DSC) was carried out using a modulated DSC unit (Model: DSC 2920, TA instrum., USA). Samples were heated in the temperature range −80 to 225 °C at a heating rate of 10 °C $min^{-1}$, in a static nitrogen atmosphere. Mechanical testing to determine the tensile strength and maximum elongation at break was performed using a computer-controlled micro-force tester (Instrom, USA, Model: 8800). The CPE film, in the form of a rectangular strip (20 mm × 10 mm) was clamped between the holders of the tensometer. The speed for the elongation test was maintained at 2 mm $min^{-1}$ for each sample under test at room temperature. Impedance studies were carried out using a computer-controlled EG&G (Princeton Applied Research, Model: 263A) potentiostat/galvanostat in conjunction with a EG&G frequency response analyzer, (FRA Model: 1025) in the frequency range 100 kHz–10 mHz. Impedance spectra of the cells were recorded using an ac signal of amplitude 20 mV interfaced with the computer with the software 'power suite'. The cells were assembled by sandwiching the CPE film between two lithium metal foils in an inert atmosphere (argon-filled glove-box with oxygen and water contents of <1 ppm (MBraun, Germany)). The electrical conductivities of the CPE films were evaluated from the ac impedance spectra of the symmetrical cells, Li | CPE | Li, as a function of temperature.

The electrochemical stability of the CPEs was determined by a sampled dc voltametry technique in which the variation of the residual electronic current of the symmetrical cells, Li | CPE | Li, was monitored as a function of the applied voltage across the cells. The resulting current–voltage characteristics gave an estimate of the maximum working voltage ($V_{max}$) (i.e. the decomposition potential) of the electrolyte, by noting the voltage at which the current rises exponentially. The ionic transport number, $t_{ion}$, was measured by means of a dc polarization technique and calculated using the equation, $t_{ion} = (i_T - i_e)/i_T$, where $i_T$ is the total ionic current and $i_e$ the residual electronic current.

## 3. Results and discussion

### 3.1. OpticaI microscopy

Optical micrographs of the $(PEO)_8$–$LiCF_3SO_3 + x$ wt.% $Li_{1.4}[Al_{0.4}Ge_{1.6}(PO_4)_3]$ system for different filler concentrations ($x$) are shown in Fig. 1a–d. The micrograph of the polymer–salt (PS) complex without the filler ($x = 0$) indicates the presence of distinct spherulites that show characteristic lamellar microstructure, Fig. 1a. The dark boundaries observed between the spherulites show the existence of an amorphous phase in the polymer film [21]. Addition of the filler causes substantial changes in the morphological features (spherulitic texture) as demonstrated in the micrographs, Fig. 1b–d. The white regions are fragmented into further smaller regions with increasing filler concentrations ($x$) and result in more disorder in the system, which thus suppresses the formation of the crystalline phase as reported by Scrosati et al. [29].

### 3.2. XRD analysis

The XRD patterns of the CPEs with various $x$ are presented in the Fig. 2a–d. Diffraction peaks which are characteristic of pure PEO are observed at $2\theta$ values of 19 and 23°. The peaks appearing at $2\theta$ values of 12, 17, 20 and 21° are attributed to the PS complex, $(PEO)_8$–$LiCF_3SO_3$ [30,31]. The d-spacings corresponding to these peaks remain almost unaffected on the addition of the filler, $x$. Further, additional peaks appear at $2\theta$ values of 25, 30, 33, 38° and at other higher angles and their intensity increases with the increasing $x$, Fig. 2a–d. These peaks have been ascribed to the

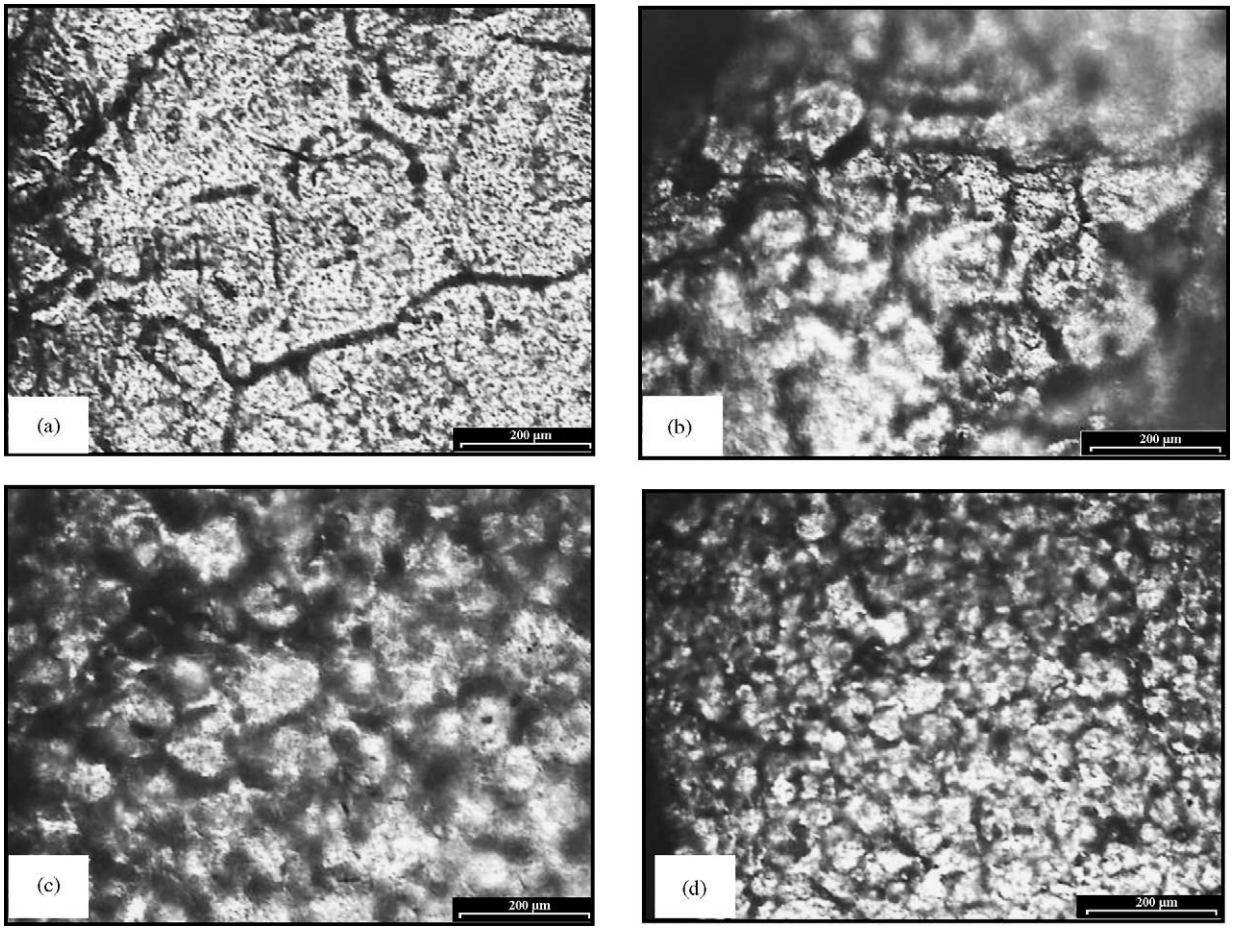


Fig. 1. Optical micrographs of CPE films $(PEO)_8$–$LiCF_3SO_3$ + $x$ wt.% filler, $Li_{1.4}[Al_{0.4}Ge_{1.6}(PO_4)_3]$, where (a) $x = 0$ wt.%; (b) $x = 2$ wt.%; (c) $x = 10$ wt.%; (d) $x = 20$ wt.%.

additive, $Li_{1.4}[Al_{0.4}Ge_{1.6}(PO_4)_3]$, as a separate phase, the XRD pattern of which is given in Fig. 2e. In addition to these features, the intensity of the peaks decreases and there is a noticeable broadening of the XRD peaks as hump formation in the range $2\theta = 15$–$50$ for CPE films with filler addition. These features are indicative of a reduction in the crystallinity of the CPE with the addition of filler. The peak-area broadening and hump formation are not seen for $x = 20$, possibly due to the agglomeration of the filler particles in the CPE, and results in decrease of the amorphous phase.

### 3.3. DSC studies

The DSC curves for CPEs with $x = 0$–$25$ wt.% are given in Fig. 3. The small step seen at $-52$ °C for all $x$ is assigned to the $T_g$. The predominant endothermic peak ($T_{m1}$) at $+50$ °C is attributed to the melting of the crystalline PEO, and the second, broad, endothermic peak ($T_{m2}$) in the range 150–190 °C is due to the melting of the salt-rich PEO–$LiCF_3SO_3$ crystalline phase [31]. The small endothermic peak at 135 °C for $x = 7.5$ and 25 wt.% (Fig. 3), is ascribed to the Li-salt present in the complex, since the DSC of the pure Li-triflate salt shows an endothermic peak at 138 °C.

Addition of the filler to the $(PEO)_8$–$LiCF_3SO_3$ complex has a noticeable influence on the $T_g$ and $T_{m2}$ values (Fig. 3 and Table 1). The $T_g$ of the CPEs increases from $-52$ °C for $x = 0$ to $-39$ °C for $x = 7.5$. Subsequent filler addition, however, systematically decreases the $T_g$ which reaches a minimum ($-51$ °C) at $x = 20$ wt.% (Table 1 and Fig. 4a). Though a systematic change is not seen, $T_{m1}$ increases by 5 °C with the addition of filler, with the exception of $x = 2$ wt.% for which $T_{m1}$ decreases to 47 °C. The melting temperature ($T_{m2}$) of the PEO-salt complex is enhanced substantially, especially at high $x$ ($\geq$15 wt.%). The flat nature of the DSC thermograms of $x = 7.5$ wt.% above $T > 150$ °C and a substantial enhancement of $T_{m2}$ for $x \geq 15$ wt.% are an indication of the improvement in the thermal stability of the CPEs.

The degree of crystallinity ($X_c$) of the CPEs has been calculated from the DSC data in terms of the ratio of the enthalpy change of the melting of the crystalline PEO in the CPE films to that of the PS complex. The variation of $X_c$ values as a function of filler concentration, $x$, is shown in Fig. 4b. It can be seen that $X_c$ decreases with filler addition

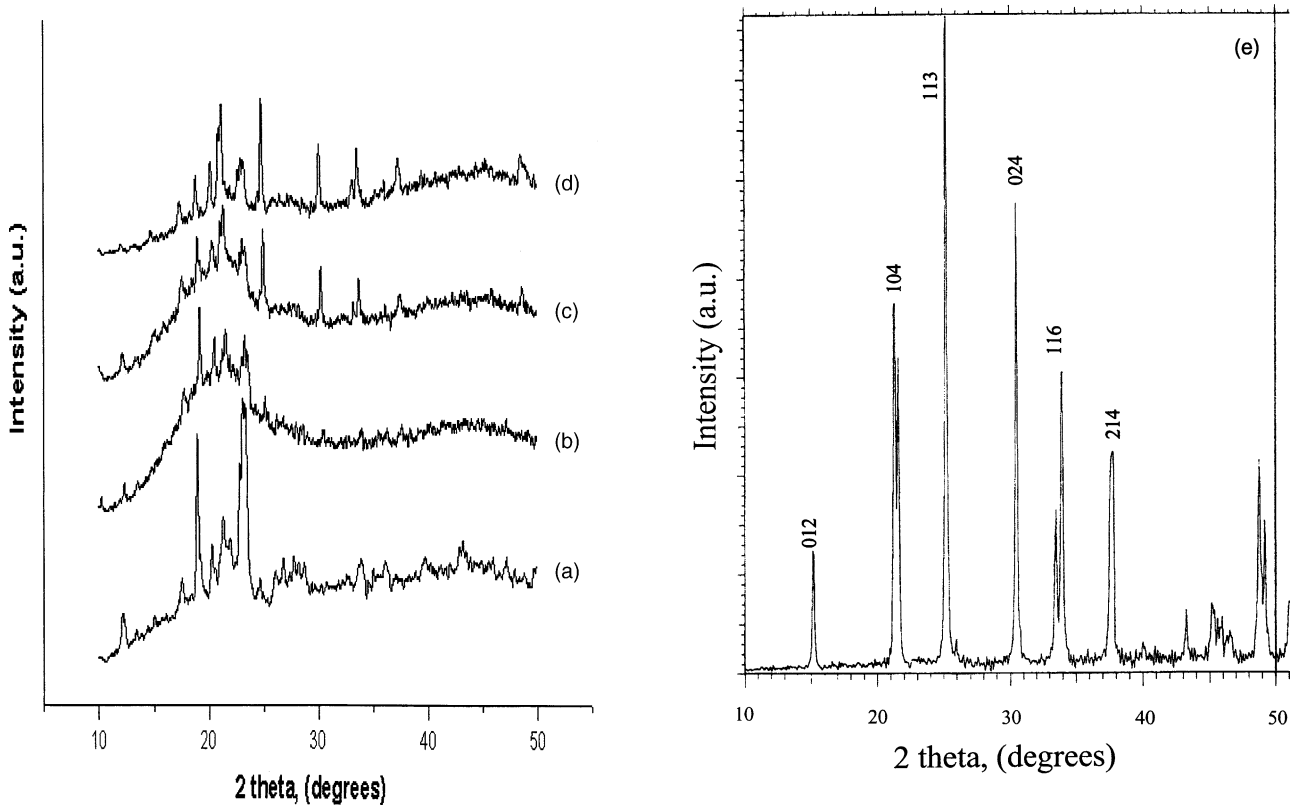


Fig. 2. XRD patterns of CPEs with filler concentrations (a) $x = 0$ wt.%; (b) $x = 2$ wt.%; (c) $x = 10$ wt.%; (d) $x = 20$ wt.%; and (e) XRD pattern of filler, $Li_{1.4}[Al_{0.4}Ge_{1.6}(PO_4)_3]$. Miller indices (*hkl*) are indicated.

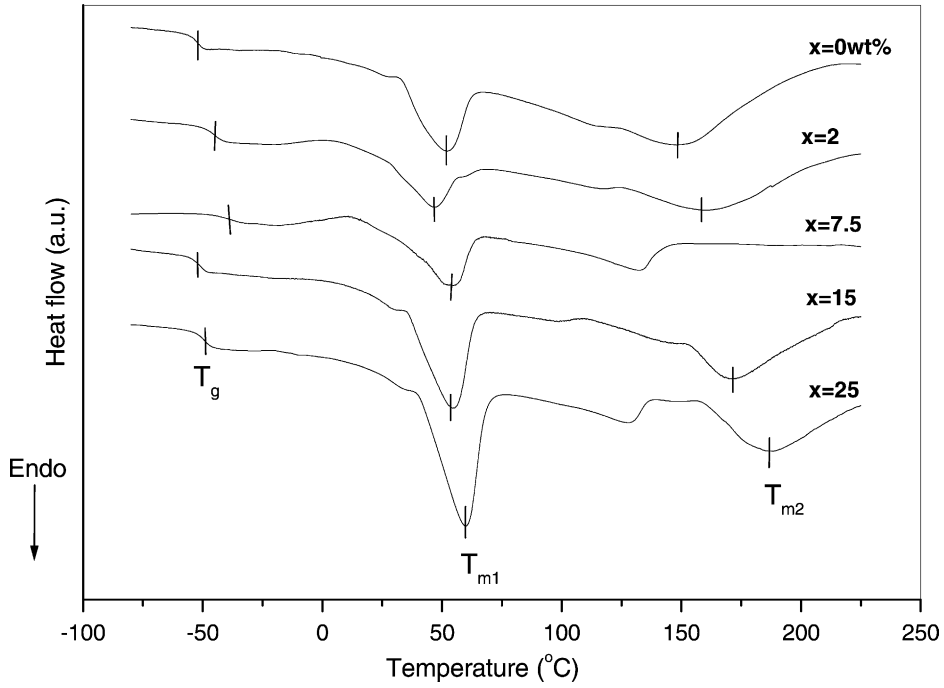


Fig. 3. DSC curves showing variation in $T_g$ and melting temperatures ($T_{m1}$ and $T_{m2}$) of CPEs with different filler concentrations ($x$).

Table 1
DSC and mechanical data of CPE films {$(PEO)_8$–$LiCF_3SO_3$ + $x$ wt.% $Li_{1.4}[Al_{0.4}Ge_{1.6}(PO_4)_3]$}

| $x$ | $T_g$ (±2 °C) | $T_{m1}$ (±2 °C) | $T_{m2}$ (±2 °C) | $\Delta H$ (of $T_{m1}$) (±5 J/g) | Mechanical parameters | |
|---|---|---|---|---|---|---|
| | | | | | Tensile strength (±0.5 MPa) | Elongation at break (±0.3%) |
| 0 | −52 | 52 | 149 | 305 | 6.8 | 12.3 |
| 1 | −50 | 57 | 165 | 260 | 7.9 | 11.7 |
| 2 | −45 | 47 | 160 | 220 | 9.0 | 10.9 |
| 5 | −42 | 58 | – | 309 | 16.9 | 9.6 |
| 7.5 | −39 | 56 | – | 235 | 20.3 | 9.2 |
| 10 | −42 | 58 | 158 | 341 | 22.8 | 10.8 |
| 15 | −50 | 55 | 170 | 374 | 12.7 | 9.4 |
| 20 | −51 | 56 | 166 | 476 | 10.9 | 7.3 |
| 25 | −50 | 60 | 187 | 528 | 12.4 | 7.4 |

up to $x = 7.5$ wt.%, with the exception of $x = 5$ for which an increase is observed. This provides insight into the characteristic role of the filler in inhibiting crystallization, which thereby reduces the volume fraction of the crystalline phase in the PS complex. This observation is in agreement with the reduction of the spherulite size and broadening of the XRD peaks of PEO with the addition of filler (Figs. 1 and 2). Further, for $x > 7.5$ wt.%, $X_c$ increases in accordance with the XRD data. A comparison of the variation of $T_g$ and $X_c$ of the CPEs with $x$ indicates that $T_g$ increases while $X_c$ decreases initially with $x$. This trend is reversed at subsequent higher filler contents ($x > 7.5$ wt.%). The featureless DSC curve for $x = 7.5$ wt.% at higher temperatures and the fact that $T_g$ is maximum with a low degree of crystallinity ($X_c$), makes this composition have the best thermal stability.

### 3.4. Electrochemical stability and transport number

The variation of residual electronic current of the cells, Li | CPE | Li, as a function of the applied voltage for the CPEs is shown in Fig. 5. The current increases gradually with increasing applied voltage up to a certain limit, namely, the 'maximum working voltage' ($V_{max}$). Beyond this voltage, the current rises abruptly. The values of $V_{max}$ for CPEs with $x = 0$, 2 and 10 are 3.18, 3.47 and 3.75 V, respectively. These results indicate an improvement in the electrochemical stability of the polymer films with the addition of filler.

The $t_{ion}$ values of the CPE with $x = 0$ and 10 wt.% were determined using Wagner's polarization technique [32]. The variation of polarization current for an applied dc voltage of 1.5 V as a function of time was measured. The $t_{ion}$ values were determined from the data in Fig. 6. A value of around 0.98 was obtained for the $t_{ion}$ of CPEs with $x = 0$ and 10 wt.%, which compares well with the values of 0.9–0.98 reported in the literature for the PEO + $KBrO_3$ system [33]. The high value of $t_{ion}$ indicates that the charge transport is predominantly ionic in both the PS complex and the CPEs.

### 3.5. Variation of conductivity with filler concentration

The dependence of the ionic conductivity ($\sigma$) of the CPE films with filler concentration $x$ wt.% at 25, 40 and 100 °C is shown in Fig. 4c–e. The $\sigma$ values were evaluated from the impedance spectra As can be seen, the $\sigma$ decreases by a factor of 2–3 with the addition of small amounts of filler ($x$) at all three temperatures. An apparent $\sigma$-maxima at $x = 2$ and 7.5 wt.% are observed, particularly in the data obtained at 25 and 40 °C. The $\sigma$ remains almost the same for $x > 7.5$ wt.% at 25 °C, whereas a decreasing trend is seen at 40 and 100 °C, Fig. 4c–e. The variation of $\sigma$ as a function of $x$ is due to changes in $T_g$ and $X_c$ caused by filler addition. The value of $T_g$ reflects the segmental motion of the polymeric chains in the amorphous phase of the electrolyte. The higher the value of $T_g$, more rigid will be the polymer matrix and, hence, the lower the mobility of the polymer chains which, in turn, lowers the $\sigma$. The value of $X_c$ provides information on the proportions of the crystalline and amorphous phases present in the polymer matrix. It is believed that the ionic motion is much better in the amorphous phase (by about three-orders of magnitude) than in the crystalline phase and, hence, an increase in the amorphous phase results in an enhancement of $\sigma$. The extent to which the $T_g$ and $X_c$ change as a result of filler addition will govern the variation of $\sigma$. As a result, $\sigma$ can vary widely as reported for a variety of CPEs [23,29,34–42].

In the present work, the $T_g$ of the PS complex ($x = 0$) is found to be lower than that of CPEs with $x \neq 0$ and hence, as expected, the $\sigma$ is high for $x = 0$ at any given temperature (Fig. 4). The $X_c$ of the PS complex is higher than that of CPEs with $x = 1$–7.5 wt.%, which tends to reduce the $\sigma$ value in comparison with those of the CPEs. Thus, as mentioned earlier, the $T_g$ and $X_c$ have an antagonistic effect on $\sigma$. This aspect has been discussed in the literature to explain the $\sigma$ of several CPEs based on the PEO system [14,43,44]. The decrease in the segmental motion of the polymeric chains of the CPEs as a result of increase in $T_g$ with $x$, with a subsequent lowering of the number of mobile charge carriers, appears to dominate over the decrease in $X_c$.

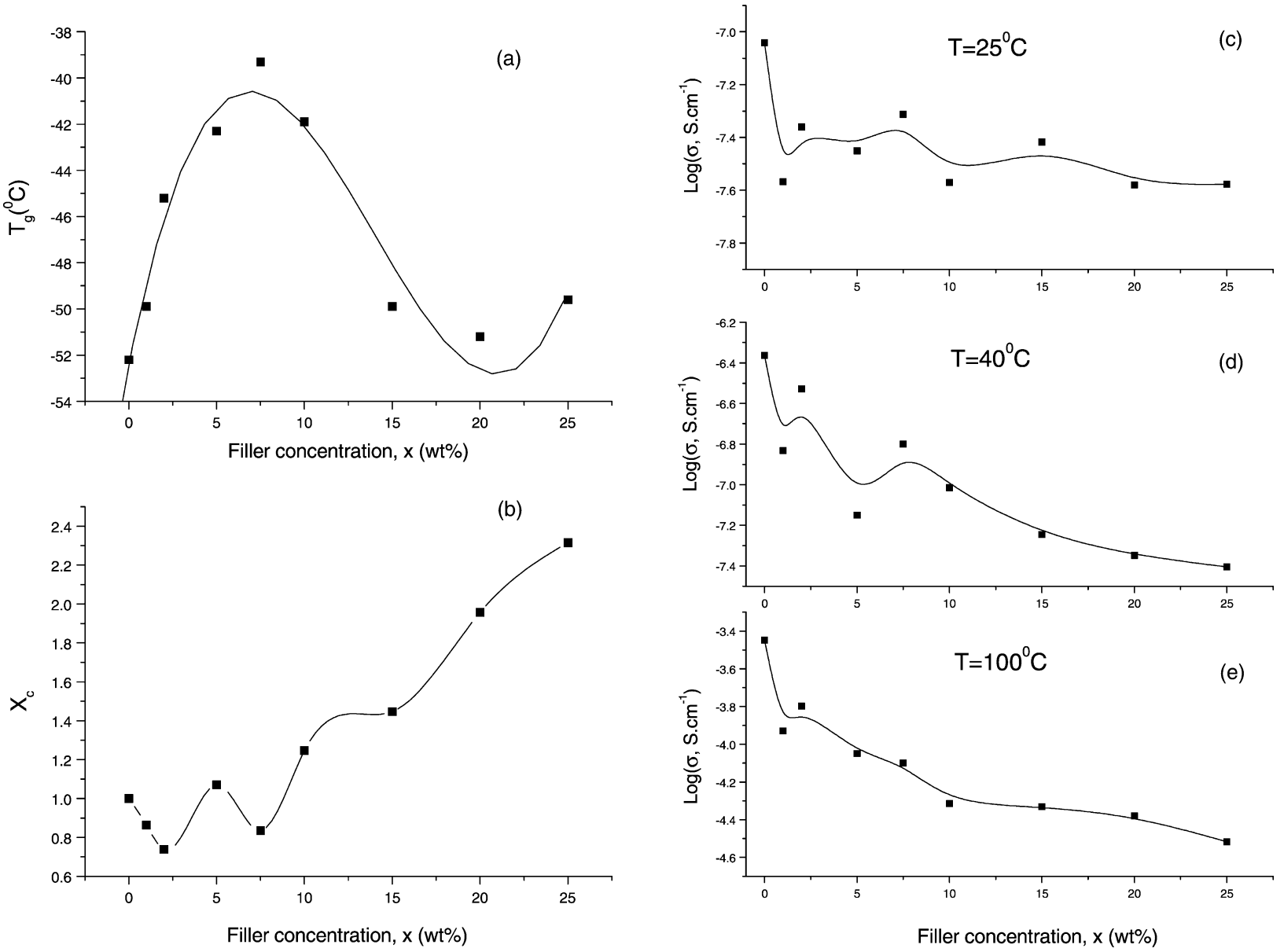


Fig. 4. (a, b) Variation of $T_g$ and $X_c$ as a function of filler concentration ($x$). (c–e) Variation of conductivity as function of $x$ at various temperatures.

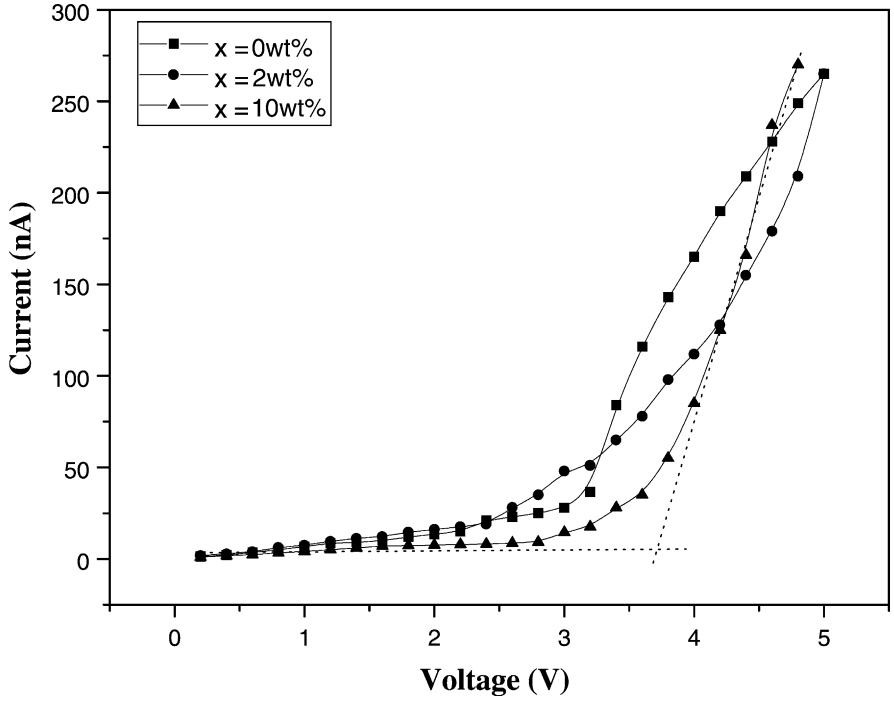


Fig. 5. Residual electronic current as function of applied voltage for CPEs with various $x$.

As a result, the $\sigma$ of the CPEs is lowered slightly compared with that of the pure PS complex ($x = 0$).

The decrease in $\sigma$ for $x > 7.5$ indicates the optimum filler content ($x$) to be between 7.5 and 10 wt.%. For $x > 10$, phase discontinuities and dilution effects result in a lowering of the $\sigma$, as reported for the $\gamma$-$LiAlO_2$–$(PEO)_8$–$LiClO_4$ system [23], and clustering or agglomeration of the filler particles may also contribute to the decrease in ionic pathways, as observed in the PEO–$LiClO_4$–SiC system [14]. Thus, the trend of the $\sigma$ variation with $x$ for present system at any temperature is attributed to the combined effect of the variation in $T_g$ and $X_c$ with $x$. The filler particle size also

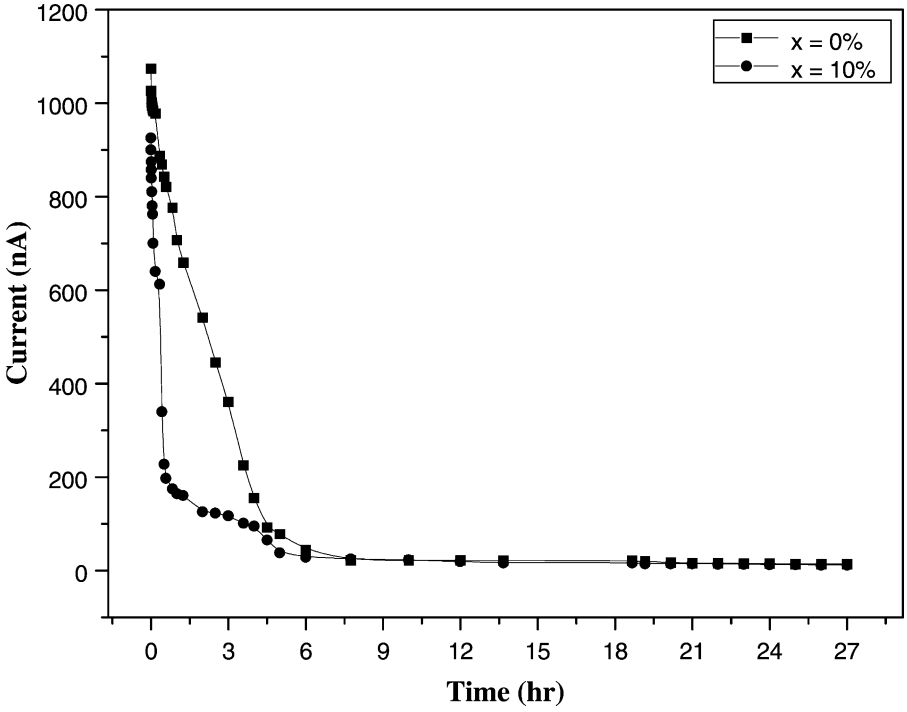


Fig. 6. Polarization current as function of time (applied voltage = 1.5 V) of CPEs with $x = 0$ and 10.

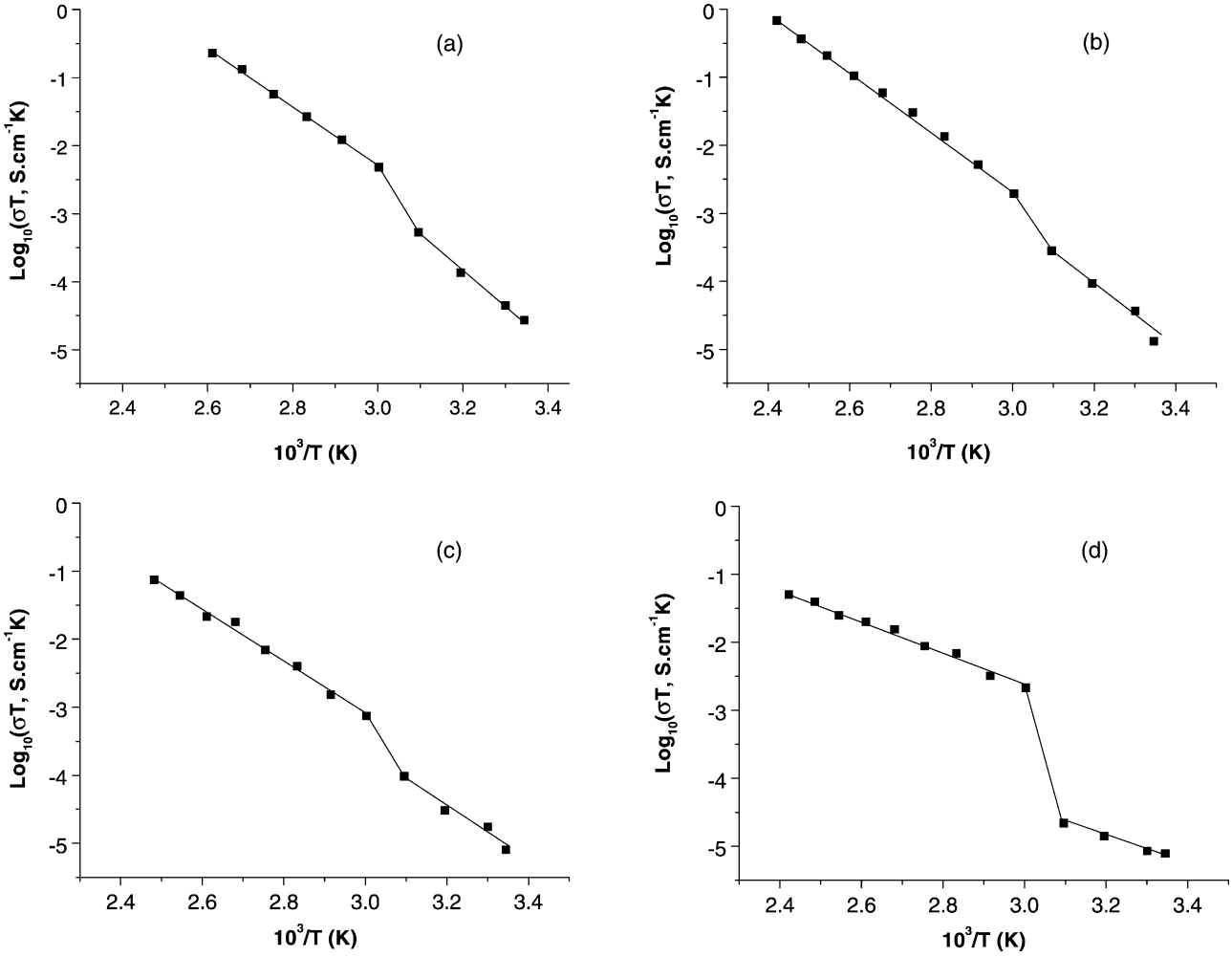


Fig. 7. Arrhenius plots ($\log_{10}(\sigma T)$ vs. $1000/T$) of CPEs with various $x$. (a) $x = 0$ wt.%; (b) $x = 2$ wt.%; (c) $x = 10$ wt.%; and (d) $x = 20$ wt.%.

appears to play a role in $\sigma$ enhancement [29,45,46], though this aspect has still to be investigated.

### 3.6. Variation of conductivity with temperature

The impedance measurements were made as a function of temperature in the range 25–400 °C, up to the maximum temperature that the samples could withstand, in steps of 10 °C for $x = 0$, 2, 10 and 20 wt.%. The conductivity values determined from the impedance plots were fitted to the Arrhenius equation, $\sigma T = \sigma_0 \exp(-E_a/k_B T)$, where $E_a$ is the activation energy, $\sigma_0$ the pre-exponential factor, $k_B$ the Boltzmann constant, and $T$ is the absolute temperature. The straight-line fit signifies an Arrhenius-type, thermally-activated process before and after the crystalline melting point ($T_{m1}$) and, accordingly, shows two $E_a$ values (Fig. 7). The discontinuity observed in the slopes at ~60 °C signifies an abrupt increase in the $\sigma$ of the CPEs. This enhancement is due to the melting of the crystalline phase of the CPEs, which occurs in the range 50–60 °C as observed by DSC (Table 1 and Fig. 3). Since the amorphous phase of the CPE has a higher $\sigma$ compared with the crystalline phase, the sudden increase in $\sigma$ observed at $\sim T_{m1}$ is as expected.

Though the addition of the filler decreases the $\sigma$, the $\sigma$–$T$ variation of the CPEs with and without the filler ($x$) does not show any qualitative change in behavior and the discontinuity at ~66 °C in the Arrhenius plots is little affected (Fig. 7). The $E_a$ and $\log_{10}(\sigma_0)$ determined from the Arrhenius plots for $T < T_{m1}$ and $T > T_{m1}$ consistently show a decrease with increase in $x$ (Table 2). The decrease in the $E_a$ values with $x$ should have resulted in an increase in the value of $\sigma$,

Table 2
Pre-exponential factors ($\log_{10}(\sigma_0)$) and activation energies ($E_a$) of CPEs before and after crystalline PEO melting temperature ($T_{m1}$)

| $x$ (wt.% filler) | $T > T_{m1}$ (25–60 °C) | | $T > T_{m1}$ (60–140 °C) | |
|---|---|---|---|---|
| | $\log_{10}(\sigma_0)$ | $E_a$ | $\log_{10}(\sigma_0)$ | $E_a$ |
| 0 | 13.1 | 1.06 | 10.6 | 0.86 |
| 2 | 9.8 | 0.85 | 10.3 | 0.85 |
| 10 | 7.3 | 0.73 | 8.3 | 0.76 |
| 20 | 2.5 | 0.46 | 4.5 | 0.47 |

provided $\log_{10}(\sigma_0)$ remained constant. The $\sigma$ decreases, however, due to the fact that $\log_{10}(\sigma_0)$ also decreases substantially with increasing $x$. Hence, despite increasing the volume fraction of the amorphous phase in the CPEs, addition of the filler decreases $\sigma$ (for $x < 10$). This is due to the negative effect of decreasing substantially the number of mobile charge carriers, either by blocking the ionic pathways or by hindering the segmental motion of the polymer chains.

### 3.7. Mechanical properties

Addition of the filler has considerable effect on the morphological characteristics of the CPE films, which has been clearly seen in the optical micrographs and the XRD data. This will have a definite bearing on the mechanical properties as well. The measured values of tensile strength (TS) and the maximum elongation at break (%) are given in Table 1. Definite improvement is observed in the TS of the CPEs relative to the undispersed PS complex ($x = 0$). The TS increases with $x$ and reaches a maximum of 22.8 MPa for $x = 10$, an increase by a factor of 3.5. With higher $x$, however, a sharp decrease in TS is observed (Table 1). The increase in TS is indicative of an enhancement in the rigidity and toughness of the CPE films. On the other hand, the % elongation at break decreases with increasing $x$, which suggests a decrease in the elasticity of the CPE films. These changes in mechanical properties signify dimensional stability of the CPEs against shocks.

## 4. Conclusions

A lithium-ion conducting composite polymer electrolyte system (CPE), $(PEO)_8$–$LiCF_3SO_3 + x$ wt.% $Li_{1.4}[Al_{0.4}Ge_{1.6}(PO_4)_3]$, $0 \leq x \leq 25$, has been synthesized in film form and characterized by XRD, optical microscopy and DSC. The electrical, electrochemical and mechanical properties have been studied. The $T_g$ of the CPEs increases with $x$ and attains a maximum value of $-39\ ^\circ C$ for $x = 7.5$, but then decreases for higher $x$. The flat nature of the DSC thermogram for $x = 7.5$ at temperatures greater than 150 °C and the substantial enhancement of $T_{m2}$ for $x > 15$ indicate an improvement in the thermal stability of the CPEs. The electrochemical stability of the CPEs is enhanced by the addition of filler; $V_{max} = 3.75$ V for $x = 10$ and is 0.57 V higher than that for the PS complex ($x = 0$). Addition of filler has a negative effect on the conductivity. The value of $\sigma$ of $1.6 \times 10^{-7}$ S cm$^{-1}$ for $x = 7.5$ at 25 °C is less by a factor of about three, than that of the PS complex ($x = 0$). The $\sigma$ versus $x$ curves at various temperature show two small maxima at $x = 2$ and 7.5. The variation of $\sigma$ with $x$ has been interpreted as due to the combined effect of the variations in $T_g$ and $X_c$ with $x$. The $\sigma$–$T$ dependence is typical of an Arrhenius-type, thermally-activated process both before and after $T_{m1}$. The $E_a$ and $\log_{10}(\sigma_0)$ values consistently show a decrease with increasing $x$. The mechanical properties improve considerably with filler addition. A maximum tensile strength of 22.8 MPa is found which is more than three times higher than that of the PS complex. Further studies are required to improve the $\sigma$ of the CPE films by the technique of plasticization and to explore, at the microscopic level, the actual mechanism involved in the ion-transport process.

## Acknowledgements

One author (AKT) acknowledges financial support from the Jawaharlal Nehru Memorial Fund, New Delhi, India for the award of fellowship to work at the National University of Singapore (NUS), Singapore. Special thanks are due to Ms. Shen Lu, IMRE, Singapore, for help in obtaining the mechanical data. The authors are also grateful for the assistance from Ms. Doreen Lai and Mr. Rasid Ali of IMRE and Mr. Karim of NUS.

## References

[1] W.E. Fenton, J.M. Parker, P.V. Wright, Polymer 14 (1973) 589.
[2] J.R. MacCallum, in: C.A. Vincent (Ed.), Polymer Electrolyte Reviews-I, Elsevier, London, 1987.
[3] J.R. MacCallum, in: C.A. Vincent (Ed.), Polymer Electrolyte Reviews-II, Elsevier, London, 1989.
[4] B. Scrosati (Ed.), Applications of Electroactive Polymers, Chapman and Hall, London, 1993.
[5] F.M. Gary, Polymer Electrolytes: Fundamentals and Technological Applications, VCH Publishers, New York, 1991.
[6] D.F. Shriver, P.G. Bruce, in: P.G. Bruce (Ed.), Solid State Electrochemistry, Cambridge University Press, Cambridge, 1989, p. 119.
[7] M. Watanabe, S.I. Oohashi, K. Sanui, N. Ogata, T. Kobayashi, Z. Ohtaki, Macromolecules 18 (1985) 1945.
[8] A.G. Ruzette, P.P. Soo, D.R. Sadoway, A.M. Mayer, J. Electrochem. Soc. 148 (2001) A537.
[9] H.R. Allock, P. Austin, P.M. Blonsky, D.F. Shriver, J. Am. Chem. Soc. 106 (1984) 6854.
[10] J.R.M. Giles, F.M. Gray, J.R. MacCallum, C.A. Vincent, Polymer 28 (1987) 1977.
[11] B.C.H. Steele, J.E. Weston, Solid State Ion. 7 (1982) 75.
[12] J. Plocharski, W. Wieczoreck, Solid State Ion. 28–30 (1988) 979.
[13] W. Wieczoreck, A. Zalewska, D. Raducha, Macromolecules 29 (1996) 143.
[14] B.K. Choi, K.H. Shin, Solid State Ion. 86–88 (1996) 303.
[15] G.B. Appetecchi, S. Passerini, Electrochim. Acta 45 (2000) 2139.
[16] J.R. MacCallum, S. Seth, Eur. Polym. J. 36 (2000) 2337.
[17] B. Kumar, L.G. Scanlon, J. Electroceram. 5 (2000) 127.
[18] S. Rajendran, T. Uma, Mater. Lett. 44 (2000) 208.
[19] K.M. Abraham, V.R. Koch, T.J. Blakley, J. Electrochem. Soc. 147 (2000) 1251.
[20] J. Fan, P.S. Fedkiw, J. Electrochem. Soc. 144 (1997) 399.
[21] S.A. Hashmi, A.K. Thakur, H.M. Upadhyaya, Eur. Polym. J. 34 (1998) 1277.
[22] M.M.E. Jacob, A.K. Arof, Polym. Eng. Sci. 40 (2000) 972.
[23] F. Capuano, F. Croce, B. Scrosati, J. Electrochem. Soc. 138 (1991) 1918.
[24] G.B. Appetecchi, S. Scaccia, S. Passerini, J. Electrochem. Soc. 147 (2000) 4448.

[25] G.B. Appetecchi, F. Croce, L. Persi, F. Ronci, B. Scrosati, Electrochim. Acta 45 (2000) 1481.
[26] S. Li, J. Cai, Z. Lin, Solid State Ion. 28–30 (1988) 1265.
[27] J. Fu, Solid State Ion. 104 (1997) 191.
[28] B.V.R. Chowdari, G.V. Subba Rao, G.Y.H. Lee, Solid State Ion. 136–137 (2000) 1067.
[29] B. Scrosati, F. Croce, L. Persi, J. Electrochem. Soc. 147 (2000) 1718.
[30] P. Lightfoot, M.A. Mehta, P.G. Bruce, Science 262 (1993) 883.
[31] D. Fauteux, J.R. MacCallum, in: C.A. Vincent (Ed.), Polymer Electrolyte Reviews-II, Elsevier, London, 1989, p. 121.
[32] J.B. Wagner, C. Wagner, J. Chem. Phys. 26 (1957) 1597.
[33] T. Sreekanth, M.J. Reddy, U.V.S. Rao, J. Power Sources 93 (2001) 268.
[34] J.R. Stevens, B.E. Mellander, Solid State Ion. 21 (1986) 203.
[35] S. Skaarup, K. West, B.Z. Christiansen, Solid State Ion. 28–30 (1988) 975.
[36] F. Croce, S. Passerini, A. Selvaggi, B. Scrosati, Solid State Ion. 40–41 (1990) 375.
[37] S. Panero, B. Scrosati, S.G. Greenbaum, Electrochim. Acta 37 (1992) 1533.
[38] F. Croce, G.B. Appetecchi, L. Persi, B. Scrosati, Nature 394 (1998) 456.
[39] B. Kumar, L.G. Scanlon, Solid State Ion. 124 (1999) 239.
[40] H.Y. Sun, Y. Takedo, N. Imanishi, O. Yamamoto, H.J. Sohn, J. Electrochem. Soc. 147 (2000) 2462.
[41] A.S. Best, J. Adebahr, P. Jacobsson, D.R. MacFarlane, M. Forsyth, Macromolecules 34 (2001) 4549.
[42] B. Kumar, J.D. Schaffer, N. Munichandraiah, L.O. Scanlon, J. Power Sources 47 (1994) 63.
[43] X. Li, S.L. Hsu, J. Polym. Sci. Polym. Phys. 22 (1984) 1331.
[44] E. Quartarone, P. Mustarelli, A. Magistris, Solid State Ion. 110 (1998) 1.
[45] W. Wieczorek, Z. Florjancyk, J.R. Stevens, Electrochim. Acta 40 (1995) 2251.
[46] J. Przyluski, M. Siekiershi, W. Wieczorek, Electrochim. Acta 40 (1995) 2101.